

GA-A24028

**OPTICAL DESIGN FOR Li BEAM ZEEMAN
POLARIMETRY MEASUREMENTS ON DIII-D**

by
T.N. CARLSTROM, D.M. THOMAS, and G. BREWIS

AUGUST 2002

DISCLAIMER

This report was prepared as an account of work sponsored by an agency of the United States Government. Neither the United States Government nor any agency thereof, nor any of their employees, makes any warranty, express or implied, or assumes any legal liability or responsibility for the accuracy, completeness, or usefulness of any information, apparatus, product, or process disclosed, or represents that its use would not infringe privately owned rights. Reference herein to any specific commercial product, process, or service by trade name, trademark, manufacturer, or otherwise, does not necessarily constitute or imply its endorsement, recommendation, or favoring by the United States Government or any agency thereof. The views and opinions of authors expressed herein do not necessarily state or reflect those of the United States Government or any agency thereof.

OPTICAL DESIGN FOR Li BEAM ZEEMAN POLARIMETRY MEASUREMENTS ON DIII-D

by
T.N. CARLSTROM, D.M.THOMAS, and G. BREWIS*

This is a preprint of a paper to be presented at the
Fourteenth Topical Conference on High Temperature
Plasma Diagnostics, July 8-11, 2002, Madison,
Wisconsin, and to be published in the *Proceedings*.

*Allied Optical, Oceanside, California.

Work supported by
the U.S. Department of Energy under
Contract No. DE-AC03-99ER54463

GENERAL ATOMICS PROJECT 30033
AUGUST 2002

ABSTRACT

Measurements of the magnetic field pitch angle are obtained from the polarization characteristics of the σ component of the Zeeman triplet of Li emission at 670.8 nm. A four element optical system images a horizontal Li beam on an array of 3 x 32, 1 mm diam. optical fibers, providing 32 spatial channels with 5 mm radial resolution in the plasma. Low Verdet constant glass is used for all optical elements near the DIII-D vessel to minimize the effects of Faraday rotation caused by stray magnetic fields. Before entering the fiber optics, the light passes through two crossed (45 degrees) photoelastic modulators (PEM) and a linear polarizer, which convert the various polarization states into an intensity modulated signal at the fundamental and 2nd harmonic of the PEM frequencies. For each spatial channel, light from a three fiber bundle is collimated and passes through a temperature tuned etalon (free spectral range, FSR = 0.3 nm; finesse, $F = 5.7$) in order to select only one σ line of the triplet. The FSR is large enough to adequately cover the expected Zeeman triplet and small enough to achieve a low bandwidth (0.06 nm) at reasonably low F . A 1.0 nm wide interference filter is used to block all but 4–5 peaks of the etalon. The light is then focussed on GaAs photo multiplier detectors. Details of the design and performance are presented.

INTRODUCTION

Knowledge of the edge current density is important in tokamak research for understanding local magnetohydrodynamic (MHD) stability, edge localized mode (ELM) behavior, and pedestal physics. Measurements of the magnetic field pitch angle, obtained from the polarization characteristics of the σ component of the Zeeman triplet of Li emission at 670.8 nm, will be used together with the magnetic equilibrium solver, EFIT, to infer the plasma edge current density on DIII-D.^{1,2} One of the challenges of this measurement is separating the σ and π components of the Li triplet, which are orthogonally polarized and only 0.03 nm apart for full field operation on DIII-D (2.1 Tesla). We have elected to use Fabry-Perot etalons for this purpose because of their high throughput and adequate performance at reasonable cost. This paper describes the design and performance of the optical system used for this measurement.

OPTICAL LAYOUT

The neutral lithium beam is injected just below the outboard midplane and viewed from directly below as shown in Fig. 1. A specially coated turning mirror and low Verdet glass lenses and vacuum window are used to relay an image of a 160 mm section of the beam ($R = 215$ to 232 cm) with a collection $F/\text{no} = 13.8$ onto a 3×32 array of 1 mm diameter silica fiber optics ($\text{NA} = 0.39$) with a magnification of 0.2 and $F/\text{no} = 2.76$. These components were chosen to minimize the polarization effects the optics contribute to the lithium resonance line emission. Several properties of the optical components are given in Table 1. A protective shutter and retractable polarizer used for calibration purposes, (not shown in Fig. 1) are mounted just above the turning mirror M1.

The linear and circular polarization states of the emitted light are converted to a signal amplitude and phase by the dual photoelastic modulators (DPEM) and linear polarizer (LP) located just outside the vacuum window, before the light is imaged on the fiber optics. The modulator axes of the two modulators are at 45 degrees, with the polarizer passing axis at 22.5 degrees with each modulator. The photoelastic modulators are resonant devices, each producing oscillating birefringence at a fixed frequency (20 kHz and 23 kHz). Only the central 51 mm of the DPEM 100 mm aperture is used in order to avoid non-uniformities near the edge. The DPEM/LP combination converts the various polarization states of the incoming light into an intensity modulated signal at the fundamental and 2nd harmonic of the DPEM frequencies.^{3,4}

Table I. Properties of the Imaging System Optical Components

Element	Size (mm)	FL (mm)	Thickness (mm)	Material	Coating	Position (mm)
Li beam	15x160	–	–	–	–	1378
M1	102x127	–	15	Fused silica	Dielectric*	108
L1	109	348	11	SFL6	AR	0
L2	90	204	11	SFL6	AR	541
L3	75	122	11	SFL6	AR	837
W	75	–	15	SFL6	AR	858
DPEM/LP	100	–	20	Fused silica		958
Image	3x32	–	–	–	–	1017

* Equal S and P polarization reflectivities at 670 nm, angle of incidence 39 ± 5.3 degrees, phase separation < 5 degrees.

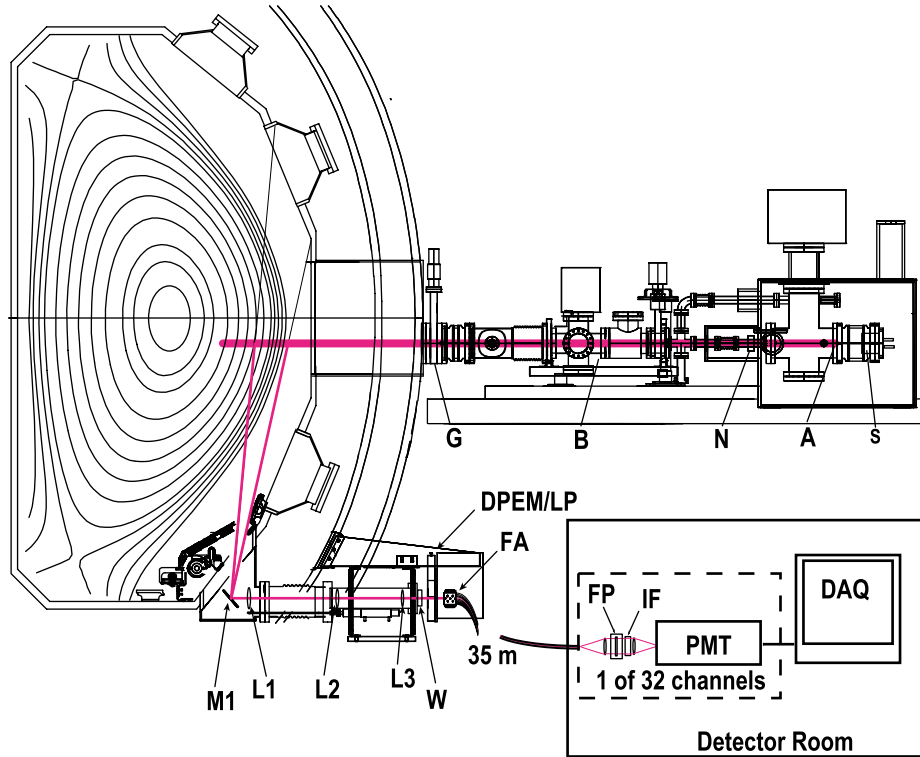


Fig. 1. Cross section of DIII-D showing the lithium beam accelerator, the viewing geometry from the bottom of the vessel, the collection optics, and the etalon and detector optics. S-source; A-accelerator; N-neutralizer; B-beamline; G-gate valve; M1-dielectric in-vessel mirror; L1-3-in-vessel collection and relay lenses; W-window; DPEM/LP-dual photoelastic modulator and linear polarizer; FA-fiber optic array; FP-Fabry-perot etalon; IF-interference filter; PMT-photomultiplier tube detector; DAQ-data acquisition system.

The fiber optics carry the signals 35 m to the detector room. Three fiber optics are combined for each spatial channel, corresponding to 5 mm radial and 15 mm toroidal resolution in the plasma. For each spatial channel, light from the 3 fiber optic bundle is collimated using a 50.8 mm diam., 100 mm focal length AR coated achromatic doublet lens. The collimated light passes through a 50.8 mm diam., 0.5 mm thick, temperature tuned etalon and a 1 nm bandpass interference filter. An identical achromatic lens focuses the light on a GaAs photomultiplier tube (Hamamatsu R636-10). The signal is amplified and filtered prior to being digitized by a PC-based data acquisition system.⁵ Details of the etalon and detector are shown in Fig. 2. The output of the etalon/interference combination when illuminated by white light is shown in Fig. 3.

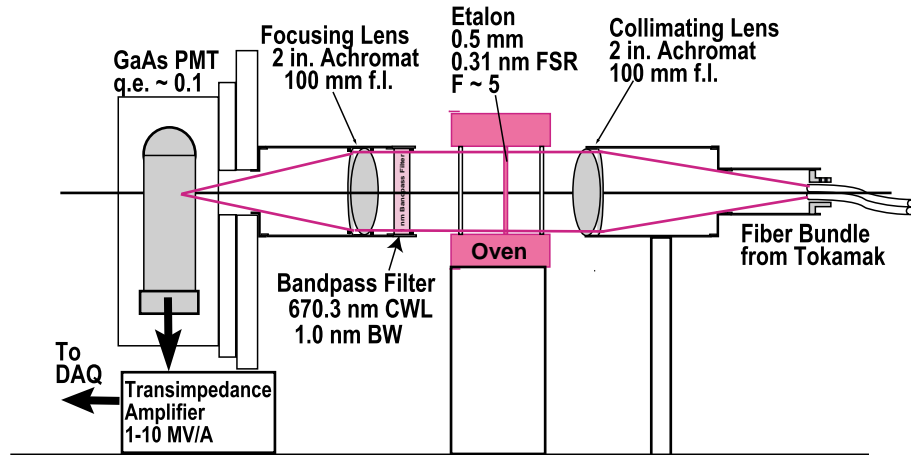


Fig. 2. Details of the etalon and detector.

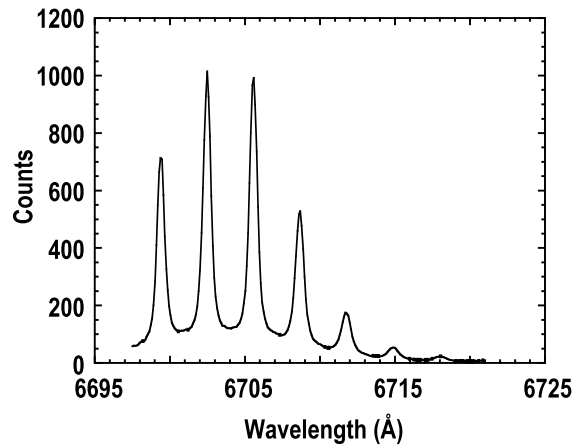


Fig. 3. Output of the etalon/interference filter pair when illuminated with white light.

ETALON

The pitch angle of the magnetic field is obtained from measurements of the polarization state of a σ component of the lithium triplet.² In order to determine the polarization state of the $\sigma +$ component, it must be separated at least partially from the orthogonal linear polarized π component and the oppositely handed circularly polarized $\sigma -$ component. This task is made difficult by the small splitting of the π and σ components (0.3 \AA for $B_T = 2.1$ Tesla on DIII-D). Due to the variation in viewing angle, each spatial channel has a slightly different wavelength caused by the Doppler shift of the 30 kV lithium neutrals. Figure 4 shows the Doppler shifted wavelength of the Li line as a function of channel number measured using a 3/4 m SPEX spectrometer with 1200 groove/mm grating operated in second order. Therefore, each channel must be tuned to the proper wavelength individually. Because of the number of spatial channels (32), a low cost resolving instrument using a Fabry-Perot etalon was investigated.

In our work to date, we have used temperature tuned fused silica solid etalons, 50.8 mm diam., 0.5 mm thick, with a surface figure of $\lambda/40$, and a reflectivity of 0.80.⁶ The free spectral range, $FSR = \lambda^2/2nd = 3.1 \text{ \AA}$, where $n = 1.45$ is the index of refraction and $d = 0.5$ mm is the thickness, and the reflectivity finesse, $F = \pi \sqrt{R/(1-R)} = 14$ where $R = 0.8$ is the reflectivity. This results in a bandwidth of 0.22 \AA , which would easily resolve the σ component. However, the finesse is reduced by the surface figure of the etalon and the fact that the light is not perfectly collimated. A surface figure finesse $F_{\text{surface}} = s/4.7 = 8.5^7$ where s is the surface figure given as a fraction of the wavelength (i.e. $s=40$ for $\lambda/40$ surface figure). The pinhole finesse, $F_{\text{pinhole}} = 4\lambda L^2/ndD^2 = 9.3$, where $L=100$ mm is the focal length of the collimating lens and $D=2$ mm is the diameter of the input fiber bundle. The resulting finesse is 5.7, determined by the inverse quadrature sum $1/F^2 = 1/F_R^2 + 1/F_{\text{pinhole}}^2 + 1/F_{\text{surface}}^2$. This results in a bandwidth of 0.57 \AA .

The etalons are mounted in small, temperature feedback controlled ovens⁸ in order to control the wavelength of the peak transmission. The shift in the peak of the etalon transmission as a function of temperature is shown in Fig. 5. The linear response has been very stable and repeatable. A measurement of the etalon transmission, obtained by temperature tuning the etalon while observing a hollow cathode lithium lamp, is shown in Fig. 6. The curve is a fit to the theoretical etalon function indicating a finesse of 5.75, which agrees fairly well with the expected performance. The low maximum transmission of 51% may be due to the reflectivity finesse, F_R , exceeding F_{surface} and F_{pinhole} .

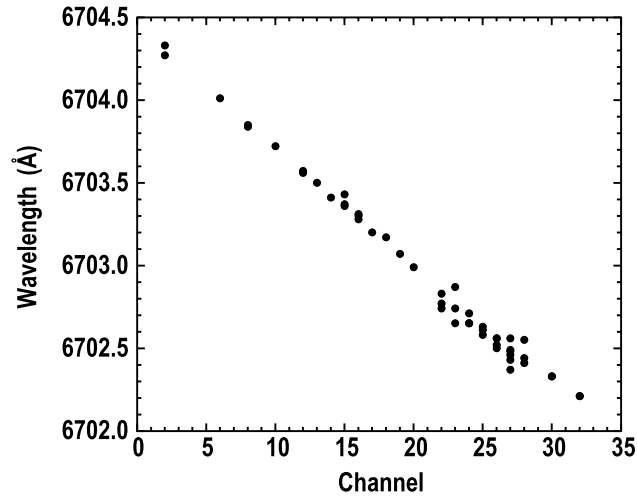


Fig. 4. Doppler shifted wavelength of the Li line as a function of channel number.

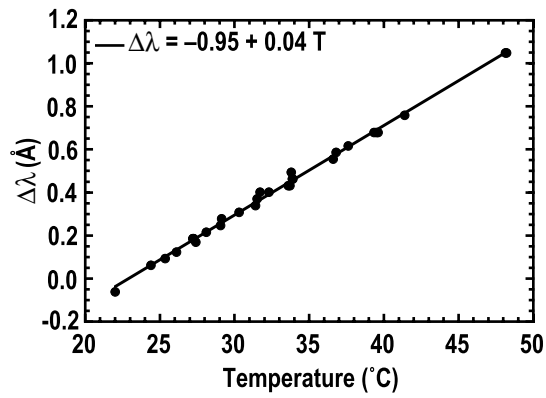


Fig. 5. Shift in the peak of the etalon transmission as a function of the oven temperature.

MODELING

We have modeled the effect of tuning the etalon across the σ line. Figure 7 shows the σ and π components broadened to FWHM of 0.5 \AA in order to estimate the effect of the finite lithium beam temperature and the variation in viewing angle, together with the etalon transmission function. Figure 8 shows the variation in the σ/π ratio as well as the σ^+/σ^- ratio as a function of the separation of the etalon peak from the central π line. The σ^+/π ratio has a maximum of 1.1 at a separation of 0.65 \AA , so the linear polarization fraction is only 10% in this case. The σ^+/σ^- ratio is about 4 at this separation, resulting in a reasonable circular polarization fraction. The normalized σ^+ signal is also shown and is at about 65% of its peak value at this separation.

In order to determine the pitch angle of the field lines in our viewing geometry, the ratio of the circular polarization fraction to the sum of the linear polarization fraction and the total intensity is required.² The present etalon resolution is too low and the line broadening is too wide for complete separation of the σ^+ and σ^- components. To overcome this, we rely on calibrations where the lithium beam is fired into neutral gas with a known magnetic field. In the future, we may explore using higher finesse etalons or interference filters to improve the circular polarization of the σ signal and reduce the requirements for precise amplitude calibrations.

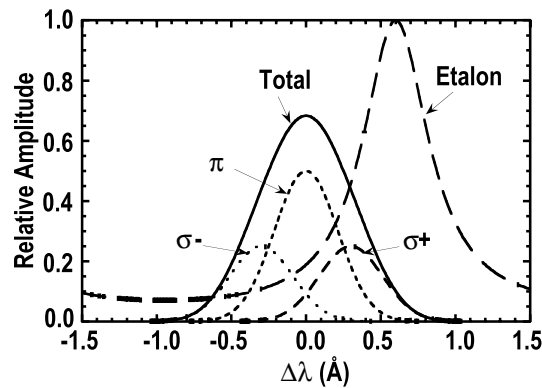


Fig. 7. Modeling of the σ and π components, broadened to FWHM of 0.5 \AA , together with the etalon transmission function.

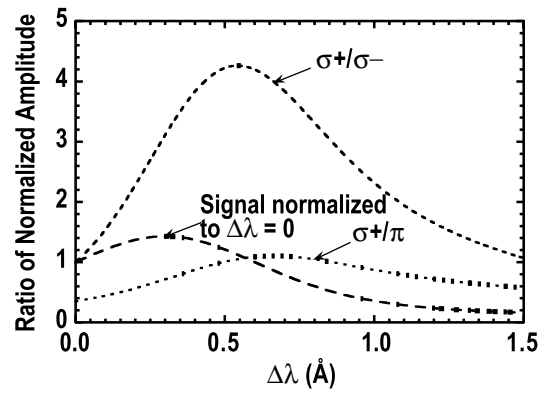


Fig. 8. Modeling of the variation in the σ/π ratio and the σ^+/σ^- ratio as well as the relative σ^+ signal as a function of the separation of the etalon peak from the central π line.

REFERENCES

- ¹D.M. Thomas, *et al.*, Rev. Sci. Instrum. **72**, 1023 (2001).
- ²D.M. Thomas, *et al.*, this conference.
- ³J.C. Kemp, Journal of the Optical Society of America, **59** 950 (1969).
- ⁴PEM-90 Photoelastic Modulator Systems User Manual, Hinds Instruments, Inc. 3175
NW Alcolek Drive, Hillsboro, OR 97124-7135
- ⁵D.K. Finkenthal, *et al.*, this conference.
- ⁶VLOC, 7826 Photonics Drive, New Port Richey, Florida 34655 USA.
- ⁷A. Title, "Fabry-Perot Interferometers as Narrow-Band Optical Filters," Harvard College
Observatory Report TR-18 (1970).
- ⁸Model ANDV8077, Andover Corp., 4 Commercial Drive Salem, NH 03079 USA.

ACKNOWLEDGMENTS

This work was supported by U.S. DOE Contract No. DE-AC03-99ER54463. The authors wish to acknowledge the technical contributions of J. Robinson, A. Bozek, J. Lynch, J. Kulchar, and S. Depaoli, and helpful discussions with Dr. A. Leonard.